Journal of Power Sources 204 (2012) 122–126

Contents lists available at SciVerse ScienceDirect

Journal of Power Sources

journal homepage: www.elsevier.com/locate/jpowsour

Short communication

# Development of ceramic sealant for solid oxide fuel cell application: Self-healing property, mechanical stability and thermal stability

Teng Zhang[a,*], Qi Zou[a], Jing Zhang[a], Dian Tang[a], Hiswen Yang[b]

[a] Institute for Materials Research, Fuzhou University, Fuzhou, Fujian 350108, China
[b] Department of Materials Science and Engineering, National United University, Miao-Li 36003, Taiwan

ARTICLE INFO

*Article history:*
Received 16 December 2011
Accepted 1 January 2012
Available online 9 January 2012

*Keywords:*
Planar solid oxide fuel cells
Self-healing
Ceramic sealant
Mechanical stability
Thermal stability

ABSTRACT

In this paper, a ceramic sealant ($CaB_2O_4$) is developed for the self-healing design of solid oxide fuel cells (SOFCs). The interface between this ceramic sealant and the anode-supported electrolyte, e.g., 8 mole% yttria-stabilized zirconia (8YSZ), remains intact after sixty thermal cycles from 800 °C to room temperature. An in situ observation verifies that the micro-indentation on the surface of this material can be healed when heating from room temperature to 920 °C at a heating rate of 40 °C min$^{-1}$. In addition, the weight loss of $CaB_2O_4$, held at 850 °C in air for 28 days, decreases from $3.26 \pm 0.73$ for sealed species to $0.81 \pm 0.04$ mg cm$^{-2}$ for fully crystallized species; meanwhile, the weight loss of $CaB_2O_4$, held at 850 °C in wet forming gas (30 vol% water vapor) for 28 days, decreases from $14.80 \pm 1.83$ for sealed species to $6.36 \pm 0.64$ mg cm$^{-2}$ for fully crystallized species. Combining with the good mechanical stability and thermal-stability, this self-healing ceramic sealant provides promising solution for the sealing challenge of planar SOFCs.

© 2012 Elsevier B.V. All rights reserved.

## 1. Introduction

Mismatch of coefficient of thermal expansion (CTE) [1–6], thermal gradient [6–8] and system configuration [9] are major sources for the generation of thermal stress in solid oxide fuel cell (SOFC) stacks. In particular, even a small CTE mismatch may result in significant thermal stresses in an SOFC stack, because of the large temperature difference between steady-operation and shutdown stages. Such thermal stresses can cause delamination and microcracking in the critical layers of the PEN [10] and degrade the SOFC performance [9,11]. Compared with glass sealants, the rigid nature of traditional ceramic sealants makes them more vulnerable to the harsh operational environment of solid oxide fuel cells (SOFCs), especially for the thermal stress accumulated during either the installment procedure or the following thermal cycles.

Recently, viscous glass-ceramics seals attract increasing attention, which release the thermal stress by the viscous flow of residual glass in the operational temperature range (e.g., 700–900 °C) of SOFCs [12–16]. The self-healing glasses are thus highly desired for the long term operation of SOFCs, e.g., at 800 °C for 40,000 h. However, most self-healing glasses are prone to crystallize under the SOFC operational condition, due to the thermodynamic instability [12]. In addition, a stopper material is required to maintain the geometric stability and structural integrity of self-healing glass sealant system, because of the overflow of self-healing glass sealants under the SOFC operational condition [17,18]. Our recent work reveals a crystalline sealant ($CaB_4O_7$) with desired self-healing behavior at about 840 °C, which provides an additional approach for achieving the sealing target of SOFCs [19]. However, the high boron content (67 mole%) leads to significant boron volatility during the crystallization process, which results in a mixture of $CaB_4O_7$ and $CaB_2O_4$.

In this paper, attention has been focused on a ceramic sealant with less boron content, *i.e.*, $CaB_2O_4$ (50 mole%), compared with that of $CaB_4O_7$ (67 mole%), to reduce the boron volatility and so that provide a more practical candidate for real application. The crystalline nature of the resulting ceramic sealant was confirmed by X-ray diffraction (XRD) and Differential Scanning Calorimetry (DSC). The self-healing behavior of this ceramic sealant was investigated using an in situ optical microscopy. In addition, the mechanical stability was evaluated by monitoring the sealing interface between ceramic sealant and an anode-supported electrolyte (8YSZ) after sixty thermal cycles. Moreover, the thermal stability of the ceramic sealant was determined by measuring the cumulative weight loss of species at 850 °C in air and wet forming gas (30 vol% water vapor) for 28 days, respectively.

## 2. Experimental

A 50-g sample of glass was prepared from a batch mixture of reagent grade calcium carbonate and boric acid to form a nominate composition of 50%CaO–50%$B_2O_3$ (in mole%). The batch was melted in a fused silica crucible in air for 2 h at 1150 °C and the melt was

* Corresponding author. Tel.: +86 591 22866540; fax: +86 591 22866537.
*E-mail address:* Tengzhangglass@gmail.com (T. Zhang).

0378-7753/$ – see front matter © 2012 Elsevier B.V. All rights reserved.
doi:10.1016/j.jpowsour.2012.01.022

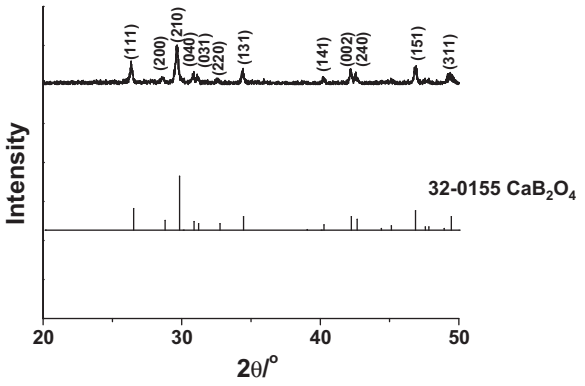


**Fig. 1.** XRD pattern of the calcium borate ceramic specimen with particle size of 45–53 μm.

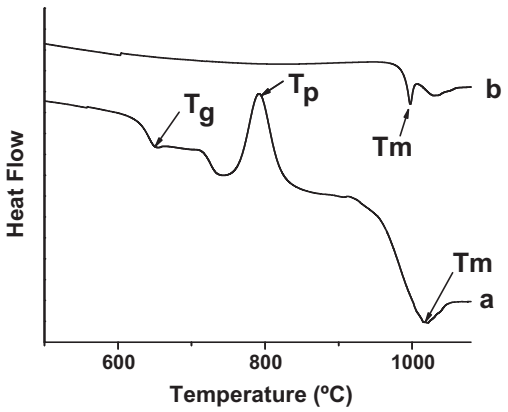


**Fig. 2.** DSC curves of the calcium borate species with particle size of 45–53 μm, for (a) quenched glass and (b) ceramic specimen.

then quenched by de-ionized water. Glass powders were crushed and sieved to 45–53 μm. The glass powders were then sealed by heating in air to 820 °C at a heating rate of 2 °C $min^{-1}$, holding for 2 h and then cooling to room temperature in furnace. Some sealed species were crystallized at 850 °C for two weeks to obtain fully crystallized species (referred to as 'ceramic species'). Some of the ceramic species were also crushed and sieved to 45–53 μm.

The crystalline phases in the ceramic powders were identified using X-ray Diffraction (XDS 2000, Scintag, Inc.) analysis, as shown in Fig. 1. The CTE of the ceramic species was measured using a dilatometer (DIL402PC, Netzsch, Inc.) at a heating rate of 5 °C $min^{-1}$. The glass transition temperature ($T_g$), crystallization temperature ($T_c$) of the glass powders and the melting point ($T_m$) of crystalline formed during the heating procedure in the DSC instrument were measured using Differential Scanning Calorimetry (SDTQ600, TA, Inc.). The DSC curve of ceramic powder, with particle size of 45–53 μm, was also collected for comparison. All DSC measurements were performed as described in a previous work [19].

Some glass powers were sealed on an anode-supported 8YSZ substrate under the same sealing condition mentioned before. The sealing couple was then holding at 850 °C for two weeks for fully crystallization. A thermal cycle includes heating sealing couple from room temperature to 800 °C at a heating rate of 40 °C $min^{-1}$, holding at 800 °C for 30 min, and then quenching in air to room temperature. The interface between ceramic sealant and the anode-supported 8YSZ after sixty thermal cycles was cross-sectioned and polished for SEM characterization (Nova NanoSEM 230, FEI, Inc.).

Some micro-indentions were created on the surface of the ceramic species using the micro-hardness tester (DHV—1000, Shanghai Jinxiang Group) at a load of 9.8 N. The in situ self-healing behavior was investigated by monitoring the change of the micro-indentations upon heating using a high temperature

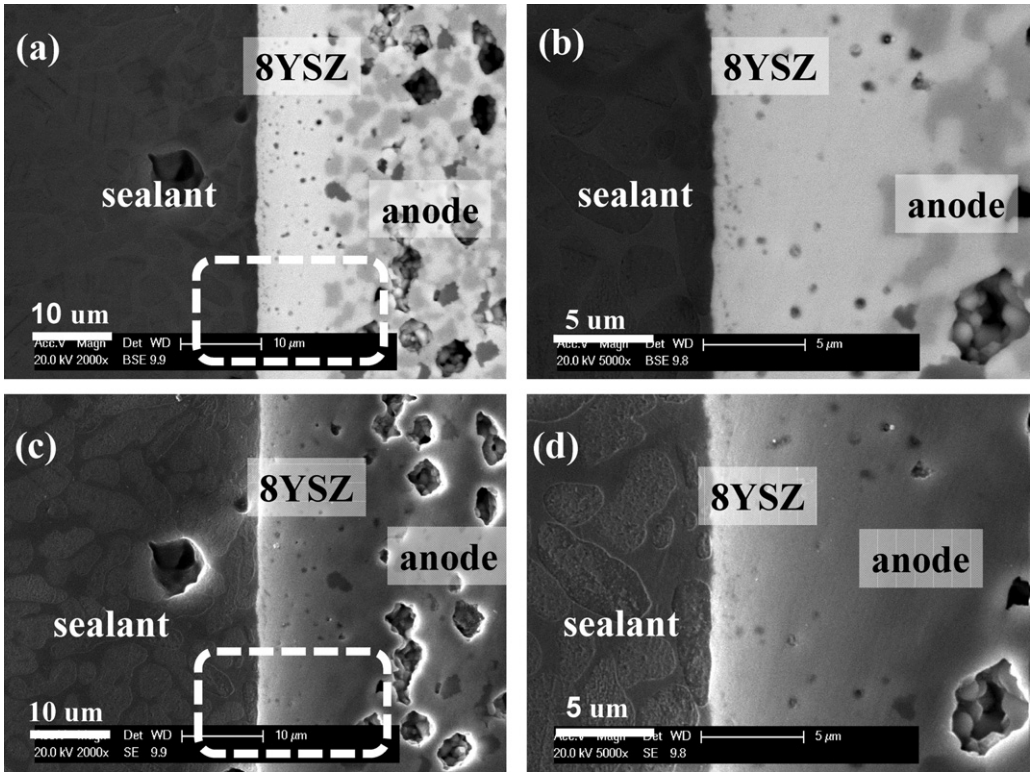


**Fig. 3.** SEM micrograph for interface between ceramic sealant and the anode-supported 8YSZ after sixty thermal cycles in air, (a) back-scattered electron image, (b) secondary electron image, (c) magnified image of indicated region in (a) and (d) magnified image of indicated region in (b).

optical microscopy (DM2500P, Leica, Inc.). The measurement was conducted from room temperature to 920 °C at a heating rate of 40 °C min$^{-1}$ and held at 920 °C for 30 min.

The measurement of weight loss is detailed in Ref. [20]. All species were polished using SiC paper (600 grit) into rectangular shapes, placed on an alumina plate and then held at 850 °C for up to 28 days under wet forming gas (10 vol% $H_2$ and 90 vol% $N_2$) with a flow rate of 10 mL s$^{-1}$. The forming gas was bubbled through deionized water held at 70 °C so that the atmosphere contained ~30 vol% water. The weight loss was measured for each specimen and the average weight loss, normalized to the glass surface area, was determined using three identical species. The weight loss in air was also measured by similar procedure for comparison.

## 3. Results and discussion

Fig. 1 shows the XRD pattern of the calcium borate ceramic specimen with particle size of 45–53 μm. The standard diffraction pattern of $CaB_2O_4$ is also included for comparison [21]. It is clear that $CaB_2O_4$ is the only crystalline phase formed in the calcium borate specimen, after the heat treatment at 850 °C in air for two weeks, which is different from the mixtures of $CaB_4O_7$ and $CaB_2O_4$ observed in previous work [19]. The absence of other borate-containing crystalline phases, such as $Ca_2B_2O_5$ and $Ca_3B_2O_6$, reveals that the crystallization schedule in present work is effective in avoiding the significant borate volatility during long term crystallization. In addition, the presence of most diffraction peaks corresponding for $CaB_2O_4$ in this specimen, e.g., (1 1 1), (2 0 0), (2 1 0), (0 4 0) and (0 3 1), confirms the crystalline nature of such ceramic species.

The DSC curves of the calcium borate species, with particle size of 45–90 μm, are shown in Fig. 2. The glass transition temperature (651 ± 5 °C) and the peak temperature of crystallization (793 ± 5 °C) in the DSC curve of the quenched glass (Fig. 2a) indicate its amorphous state; the absence of the glass transition temperature and crystallization exothermic peak in the DSC curve of the ceramic specimen (Fig. 2b), after the heat-treatment at 850 °C in air for two weeks, confirms that the specimen has been fully crystallized. The melting point of the crystalline phase, formed in the quenched glass during the heating procedure in the DSC instrument, is close to that of the crystalline phase in the ceramic specimen after fully crystallization (1017 ± 5 °C vs. 1000 ± 5 °C), indicating that the crystalline phase does not change after the long term crystallization. Combining with the XRD pattern (in Fig. 1a), the melting process observed in the DSC curves can be assigned to the only crystalline phase, $CaB_2O_4$, in present work.

Fig. 3 shows the micrograph of the interface between ceramic sealant and the anode-supported 8YSZ after sixty thermal cycles. The clean interface between ceramic sealant and the dense 8YSZ in back-scattered electron mode (Fig. 3a) and secondary electron mode (Fig. 3c) indicates that the good chemical compatibility of this ceramic sealant with electrolyte. In spite of the large CTE difference between ceramic sealant and 8YSZ (7.0 K$^{-1}$ vs. 10.0 × 10$^{-6}$ K$^{-1}$), no cracks can be observed in the magnified images of the interface after

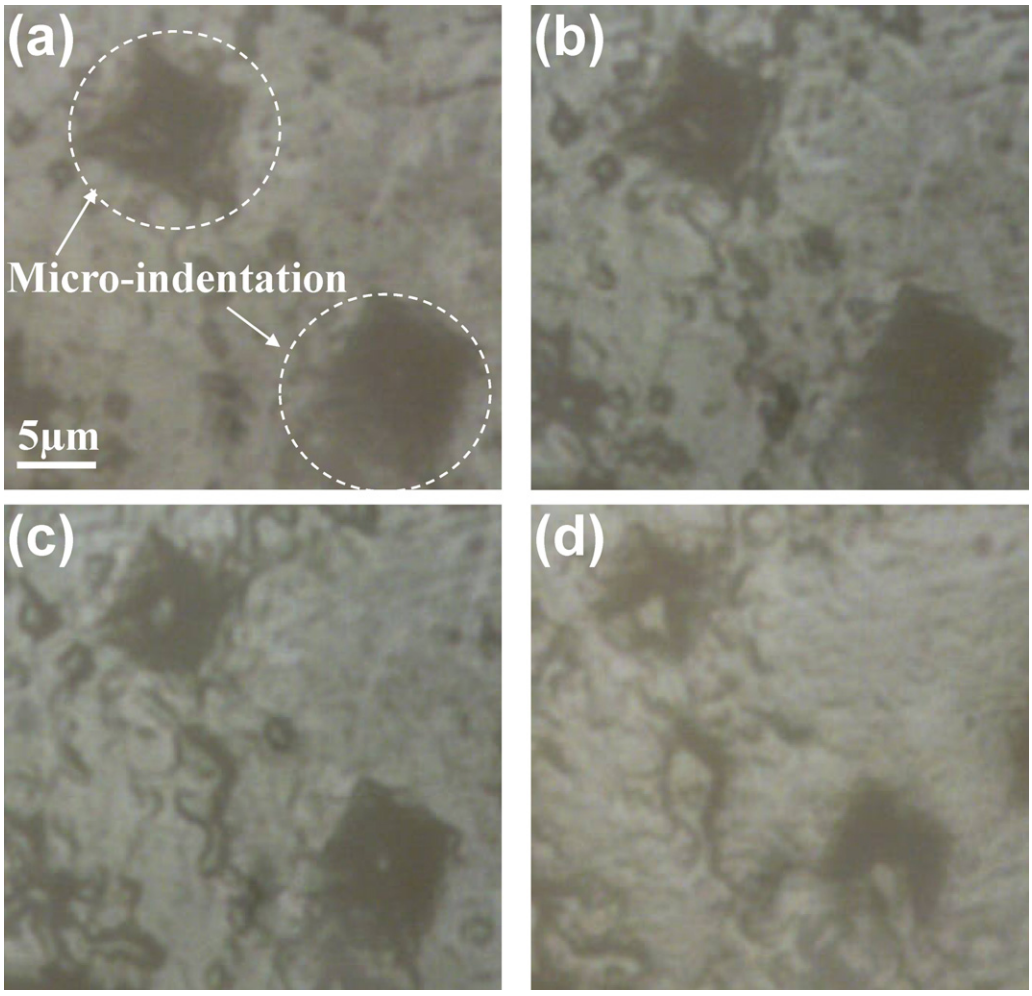


**Fig. 4.** In situ optical images of the calcium borate ceramic specimen, for (a) 820 °C, (b) 890 °C, (c) 920 °C and (d) 920 °C for 4 min.

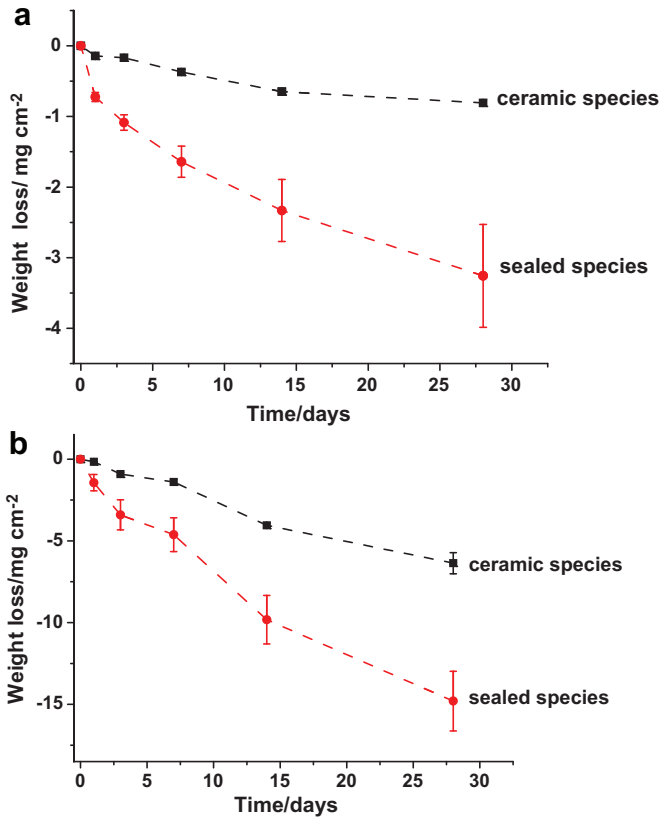


**Fig. 5.** The weight change of the calcium borate species at 850 °C for 28 days, (a) in air and (b) in wet forming gas (30 vol% water vapor). The dashed lines are guides for eyes.

sixty thermal cycles (in Fig. 3b and d). It is also worth noting that the thermal cycles in present work were carried out in a more harsh way (about 90 min) than that of other works in literature, e.g., 500 h for one thermal cycle [22]. Therefore, the $CaB_2O_4$ ceramic sealant exhibits good mechanical stability in present work, since cooling step to room temperature is found to be the most aggressive one in terms of creating high stress at the sealing interface [14].

Fig. 4 shows the change of the micro-indentations on the surface of ceramic sealant upon heating, monitored by a high temperature optical microscopy. It is clear that some micro-indentations, marked by the dash-line circle, keep shrinking when the temperature increases from 820 °C (Fig. 4a) to 890 °C (Fig. 4b) and to 920 °C (Fig. 4c). In addition, the blunting of micro-indentations tips is obvious upon heating from 820 °C to 920 °C. Finally, the spherodization of the micro-indentations can be observed when holding at 920 °C for 4 min (Fig. 4d), indicating that such ceramic specimen can be self-healed immediately under this condition, e.g., 920 °C for 4 min in present work. The self-healing behavior of this ceramic sealant can be correlated with the visco-elastic flow of $CaB_2O_4$ crystalline at temperatures close to its melting point; the tiny amount of residual glass, if presents, is not enough for inducing the observed self-healing process, considering the absences of glass transition and crystallization behaviors in the corresponding DSC curve (in Fig. 2). The visco-elastic flow of $CaB_2O_4$ also contributes to the good mechanical stability of such sealant, which releases the thermal stress and therefore avoids the initialization of cracks at the sealing interface during thermal cycles (in Fig. 3).

The cumulative weight loss of calcium borate species at 850 °C in air and wet forming gas (30 vol% water vapor) as a function of time is shown in Fig. 5. The weight loss of ceramic species in both oxidizing and reducing atmospheres accumulates at a decreasing rate when the heat-treatment time increases, in agreement with the diffusion-controlled characteristic of boron volatility [20]. The weight loss of $CaB_2O_4$, held at 850 °C in air for 28 days, decreases from $3.26 \pm 0.73$ for sealed species to $0.81 \pm 0.04\,mg\,cm^{-2}$ for ceramic species. In addition, the weight loss of $CaB_2O_4$, held at 850 °C in wet forming gas (30 vol% water vapor) for 28 days, decreases from $14.80 \pm 1.83$ for sealed species to $6.36 \pm 0.64\,mg\,cm^{-2}$ for ceramic species. The improvement in the thermal stability of ceramic specimen can be attributed to the crystallization of borate-containing phase, i.e., $CaB_2O_4$, wherein the volatile species (Boron) are blocked by numerous grains (in Figs. 1 and 3).

Boron is well known for improving the sealing properties of glasses, e.g., the dramatic reduce in the glass transition temperature ($T_g$) as well as the softening temperature ($T_d$) [23]. However, it is also notorious for high volatility from glasses at high temperature, especially with the presence of water vapor [20,24]. Therefore, the maximum borate content in sealing glasses should be 10 mole% or less to reach a compromise between the sealing properties and volatility (or thermal stability). The finding of self-healing $CaB_2O_4$ crystalline sealant, combining with good mechanical stability and improved thermal stability, provides a novel design for performing the sealing target: the glass matrix with sufficient borate content provides desired sealing properties for joining process, e.g., low $T_g$ and $T_d$; the borate-containing crystalline phase, $CaB_2O_4$, formed by controlled crystallization from the glass matrix, fulfills the self-healing requirement in routine operation of SOFCs. In addition, the good mechanical stability of this ceramic sealant can also attributed to the visco-elastic flow of the $CaB_2O_4$ crystalline, which releases the thermal stress generated during thermal cycles and results in the crack-free interface between sealant and the anode-supported electrolyte. Moreover, the relative lower boron content of $CaB_2O_4$, compared with that of $CaB_4O_7$ in previous work [19], makes it more feasible to be incorporated into a traditional rigid sealant system, which possesses the desired structural integrity of the sealing system [25].

## 4. Conclusions

The borate-containing crystalline phase, $CaB_2O_4$, exhibits a self-healing property upon heating from room temperature to 920 °C at a heating rate of 40 °C min$^{-1}$. In addition, the sealing couple of ceramic sealant/anode-supported 8YSZ shows good mechanical stability during sixty thermal cycles, due to the visco-elastic flow of such sealant. Moreover, the formation of borate-containing crystalline phase contributes to the improved thermal stability in both oxidizing and reducing atmospheres, due to the block of the volatile boron by numerous grains. The finding in this crystalline phase provides new insights into the integration of self-healing property, mechanical stability and thermal stability of sealants, which will expediate the commercialization of planar SOFCs.

## Acknowledgements

The authors gratefully acknowledge the financial support of the National Natural Science Foundation of China (No. 51102045), the Ph.D. Programs Foundation of Ministry of Education of China (No. 20103514120006), funds for Distinguished Young Scientists from the Fujian Education Department (No. JA11007) and the funding (type A) (No. JA09020) from the Fujian Education Department of China. They would also like to thank Yi Liu and Wei Xie for assistance with sample preparation, Zhenhuan Zheng for assistance with X-ray diffraction, Bingliang Liang and Jing Cao for assistance with DSC, Yannan Lin for useful discussion.

## References


[1] W. Li, K. Hasinska, M. Seabaugh, S. Swartz, J. Lannutti, J. Power Sources 138 (2004) 145–155.
[2] W.N. Liu, X. Sun, M.A. Khaleel, J.M. Qu, J. Power Sources 192 (2009) 486–493.
[3] C.-K. Lin, T.-T. Chen, Y.-P. Chyou, L.-K. Chiang, J. Power Sources 164 (2007) 238–251.
[4] L. Liu, G.-Y. Kim, A. Chandra, J. Power Sources 195 (2010) 2310–2318.
[5] J. Malzbender, J. Eur. Ceram. Soc. 30 (2010) 3407–3413.
[6] B. Kuhn, E. Wessel, J. Malzbender, R.W. Steinbrech, L. Singheiser, Int. J. Hydrogen Energy 35 (2010) 9158–9165.
[7] T.L. Jiang, M.-H. Chen, Int. J. Hydrogen Energy 34 (2009) 8223–8234.
[8] L.-K. Chiang, H.-C. Liu, Y.-H. Shiu, C.-H. Lee, R.-Y. Lee, Renew. Energy 33 (2008) 2580–2588.
[9] C.-K. Lin, L.-H. Huang, L.-K. Chiang, Y.-P. Chyou, J. Power Sources 192 (2009) 515–524.
[10] A. Selçuk, G. Merere, A. Atkinson, J. Mater. Sci. 36 (2001) 1173–1182.
[11] T. Zhang, Q. Zhu, W.L. Huang, Z. Xie, X. Xin, J. Power Sources 182 (2008) 540–545.
[12] K. Lu, M.K. Mahapatra, J. Appl. Phys. 104 (2008) 074910.
[13] A. Flügel, M.D. Dolan, A.K. Varshneya, Y. Zheng, N. Coleman, M. Hall, D. Earl, S.T. Misture, J. Electrochem. Soc. 154 (2007) B601–B608.
[14] W.N. Liu, X. Sun, M.A. Khaleel, J. Power Sources 196 (2011) 1750–1761.
[15] W. Liu, X. Sun, M.A. Khaleel, J. Power Sources 185 (2008) 1193–1200.
[16] Y.-S. Chou, E.C. Thomsen, J.P. Choi, J.W. Stevenson, J. Power Sources 197 (2012) 154–160.
[17] W.N. Liu, X. Sun, M.A. Khaleel, J. Power Sources 196 (2010) 1750–1761.
[18] N. Govindaraju, W.N. Liu, X. Sun, P. Singh, R.N. Singh, J. Power Sources 190 (2009) 476–484.
[19] T. Zhang, D. Tang, H. Yang, J. Power Sources 196 (2010) 1321–1323.
[20] T. Zhang, W.G. Fahrenholtz, S.T. Reis, R.K. Brow, J. Am. Ceram. Soc. 91 (2008) 2564–2569.
[21] Joint Committee on Powder Diffraction Standards, International Centre for Diffraction Data, Swarthmore, USA, 2001.
[22] F. Smeacetto, A. Chrysanthou, M. Salvo, T. Moskalewicz, F. D'Herin Bytner, L.C. Ajitdoss, M. Ferraris, Int. J. Hydrogen Energy 36 (2011) 11895–11903.
[23] J.W. Fergus, J. Power Sources 147 (2005) 46–57.
[24] M.J. Snyder, M.G. Mesko, J.E. Shelby, J. Non-Cryst. Solids 352 (2006) 669–673.
[25] P.A. Lessing, J. Mater. Sci. 42 (2007) 3465–3476.